Ferromagnetic metal conversion directly from two-dimensional nickel hydroxide

Yuhsuke Naruo[1], Seita Uechi[1], Masahiro Sawada[2], Asami Funatsu[3], Fuyuki Shimojo[3], Shintaro Ida[3], Masahiro Hara[3]*

[1] Graduate School of Science and Technology, Kumamoto University, Kumamoto 860-8555, Japan

[2] Hiroshima Synchrotron Radiation Center, Hiroshima University, Hiroshima 739-0046, Japan

[3] Faculty of Advanced Science and Technology, Kumamoto University, Kumamoto 860-8555, Japan

*Corresponding author. E-mail: mhara@kumamoto-u.ac.jp (Masahiro Hara)

ABSTRACT

 We have demonstrated a direct metallic conversion from nickel hydroxide nanosheets to nickel metal nanostructures by thermal annealing in vacuum. The metal transition of the single-layer nanosheets deposited on a Si substrate was revealed by X-ray absorption near edge structure (XANES) measurements. The XANES signal significantly changed at annealing temperatures above 250 ℃. The metal transition temperature coincides with the reported temperatures at which layered nickel hydroxide nanosheets are converted to nickel oxide nanosheets by calcination in air. Auger measurements confirmed that a dissociation of oxygen from the hydroxide nanosheet induces the metallic conversion. The converted nickel metallic structures exhibit ferromagnetic behavior revealed by X-ray magnetic circular dichroism (XMCD) measurement. Atomic force microscopy measurements indicate that diffusions of nickel atoms on the substrates leads to a structural change from a 2D-like structure to a particle-like structure.

Introduction

Two-dimensional (2D) materials have attracted great interest due to characteristic physical/chemical properties compared to bulk materials. Furthermore, hetero-structures by stacking different 2D materials show new functions and can be applied to future nano-devices [1,2]. A large number of 2D materials obtained from layered bulk crystals by various exfoliation methods have been reported in the last two decades. However, pure metals and their alloys including ferromagnetic metals such as Fe and Ni, do not have layered structures and cannot be exfoliated into atomic layers by the general exfoliation methods [3]. Chemically synthesized metallic 2D materials have also attracted much attention as novel catalytic materials [4,5]. Various types of 2D transition metal dichalcogenides (TMDCs) including metallic materials are exfoliated from layered TMDCs and are also created by chemical vapor deposition (CVD) methods. Although most of the metallic 2D materials are unstable in ambient air, they are demanded as potential electronic materials for future flexible devices [6].

Another root to obtaining 2D metal structures is reduction from 2D oxide materials. It is well known that transition metal oxides and hydroxides nanosheets are exfoliated from the layered metal oxides and hydroxides in chemical solutions [7]. Ruthenium (Ru) and Platinum (Pt) metal nanosheets are obtained from oxide nanosheets by hydrogen/chemical reduction methods [8,9]. Chemically obtained nickel hydroxide $Ni(OH)_2$ nanosheets with lateral size of a several hundred nanometers [10] are converted to nickel oxide nanosheets by thermal decomposition [11]. Subsequently, the nickel oxide nanosheets are also converted to metallic states by a hydrogen reduction [12]. In the metallic conversions from monolayer oxides, evaluations of metallization are rather difficult due to the ease of re-oxidations. In this paper, we report a direct conversion from $Ni(OH)_2$ monolayer nanosheets into ferromagnetic nickel metal 2D-like structures by

3

thermal annealing under vacuum. The metal transitions are evaluated by in-situ element-specific X-ray absorption spectroscopy at ultra-high vacuum (UHV) to avoid surface oxidation. To our best knowledge, this study is the first report of a metallic conversion directly from a monolayer hydroxide. The simple conversion method is also applicable for other types of monolayer hydroxide nanosheet [13,14]. Furthermore, the converted 2D-like nickel metal exhibits a ferromagnetic behavior, which can be applied to future spintronics devices composed of 2D materials.

Experimental

Ni(OH)$_2$ nanosheets were exfoliated from layered nickel hydroxides intercalated with dodecyl sulfate ions [10]. Figure 1 (a) is a structural model of Ni(OH)$_2$ nanosheet. Electronic and
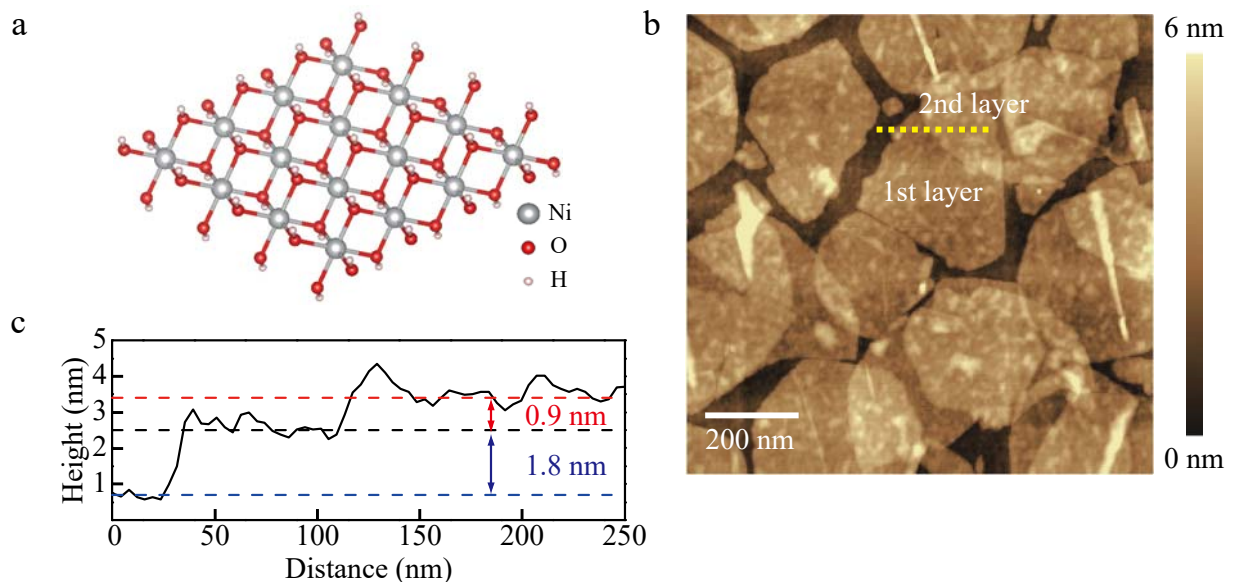
Figure1. (a) Structural model of Ni(OH)$_2$ nanosheet. (b) Atomic force microscopy image of Ni(OH)$_2$ nanosheets deposited on a Si substrate. (c) Height profile along the dashed line marked in (b).

magnetic properties in the nickel hydroxide nanosheets have been studied by simulations based on first-principles calculations [15-19]. Figure 1(b) shows an atomic force microscopy image of the nanosheets deposited on a highly doped conductive Si substrate by the Langmuir-Blodgett method. Ripples observed in Fig. 1(b) are due to water molecules or dodecyl sulfate ions trapped between the nanosheets and the Si substrate. Figure 1(c) shows the cross section of the AFM image at the dashed line in Fig. 1(b). The height between the Si substrate and the 1st layer generally increases due to surface condition such as the surface roughness. The height between the 1st layer and 2nd layer is about 0.9 nm, which is comparable to the value reported in the previous study [10]. Interlayer distance of nickel hydroxide α-Ni(OH)$_2$ and β-Ni(OH)$_2$ are 0.81 nm and 0.46 nm, respectively [20,21]. The observed height is comparable to the value of water intercalated α-Ni(OH)$_2$. This indicates presence of water molecules between the stacked nickel hydroxide nanosheets in ambient air.

In order to investigate electronic states in the nickel hydroxide nanosheets, X-ray absorption near edge structure (XANES) were measured at the BL-14 beam line of HiSOR. The measurement setup is schematically drawn in Fig. 2(b). The measured X-ray absorption corresponds to excitations from 2p core levels to 3d unoccupied levels. The spectra Ni L_2 and L_3 edges of Ni were taken in total electron yield mode by measuring the current due to X-ray absorption thorough the conductive Si substrate. The directions of the incident X-ray beam and the external magnetic field of 1.1 T supplied by a permanent magnet array were perpendicular to the substrate. The degree of X-ray circular polarization was estimated to be about 70 %. Thermal annealing for 30 minutes at different temperatures and subsequent XANES measurements at room temperature were carried out in the UHV chamber of the beam line. The pressure of the chamber was about 1×10^{-7} Pa under XANES measurements and increased up to 2×10^{-5} Pa during

thermal annealing.　XANES spectra and X-ray magnetic circular dichroism (XMCD) spectra were obtained from the average and the deviation between the X-ray absorption spectra under the oppositely directed magnetic fields.

Results and discussion

　Figure 2 (a) shows the X-ray absorption spectra for different settings of the annealing temperature. The as grown sample exhibited multiple structures corresponding to the transition $2p^63d^8 \rightarrow 2p^53d^9$, which indicates that the nickel hydroxide has valence state of Ni^{2+} [22,23]. The sample annealed below 200 °C also exhibited similar structures which indicate that the hydroxide nanosheets kept the initial structure under the low temperature annealing. Above 250 °C, the multiple structure drastically changed into two broad metallic peaks with a step-like background similar to spectra observed in a nickel single crystal [24] and deposited nickel metal films on different substrates [25-27]. Specific satellite peaks at ~ 6 eV above the L_3 main peaks are also visible as same as the earlier studies. The result indicates that the nickel hydroxide nanosheets are converted to nickel metal structures by thermal annealing under vacuum. Comparing between the two metallic spectra, the sample annealed at 250 °C has a broader main peak and a smaller 6 eV satellite peak as shown in the inset of Fig. 2(a). A similar trend was observed in deposited nickel films by reducing the thickness down to monolayer [27]. We can imagine that monolayer nickel islands are produced at the low temperature annealing, however, further investigations are needed for precise control of the nickel metal structure.
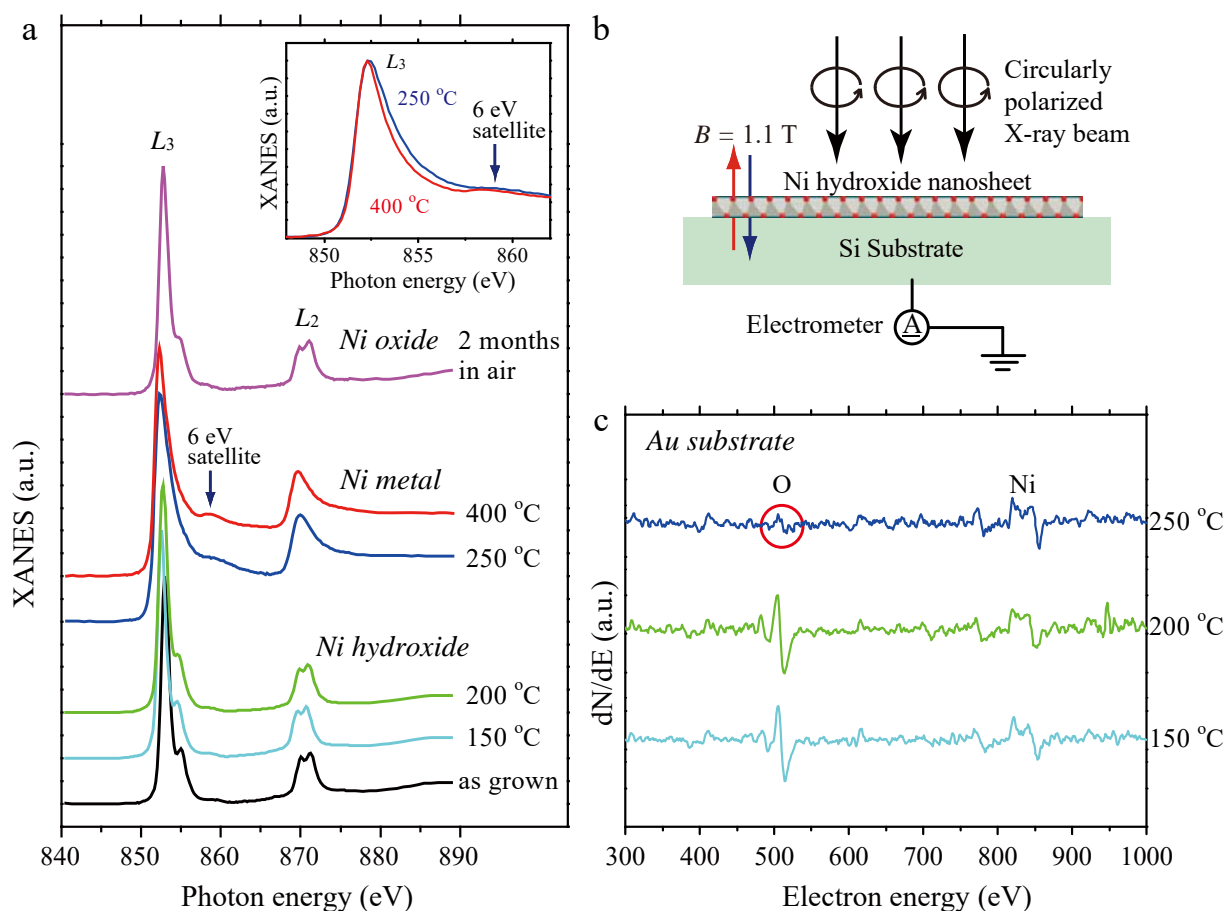
Figure2. (a) X-ray absorption near edge structure (XANES) for different annealing temperatures. Small linear backgrounds are subtracted, and different offsets are added for easy comparison. The position of 6 eV satellite peak is marked the arrow. Inset: Enlarged XANES spectra around L_3 peak for the samples annealed at 250 °C and 400 °C. (b) Schematic illustration of the X-ray absorption measurement. (c) Auger electron spectra of the $Ni(OH)_2$ nanosheets deposited on Au substrates for different annealing temperatures. The red circle indicates a small Auger signal of oxygen at 250 °C.

The converted metallic sample annealed at 400 °C was exposed to air and was measured X-ray adsorption spectra again after 2 months. The metallic broad spectra changed into a multiple structure similar to the initial hydroxides. However, additional thermal annealing in vacuum failed to convert the air-exposed sample to a metallic state. It is noteworthy to mention that layered nickel hydroxides are decomposed to nickel oxides by a calcination in air. The transition temperature from the hydroxides to the oxides is between 250 °C and 350 °C [28-32], which

coincides with the transition temperature in this experiment. Recently, nickel hydroxides nanowalls have been successfully converted to nickel metal nanosheets with 10 atomic layers by a solution-based chemical reduction [33]. In our experiment, we demonstrate that the monolayer nickel hydroxides nanosheets are successfully converted to not oxides but metallic states by a thermal annealing in vacuum, although the converted metal structures are easily oxidized by an exposure to air.

We measured Auger spectra in the annealing process to confirm the metallic transition. For avoiding signals from native oxide-layer in the Si substrates, we prepared samples in which Au films were deposited between the Si substrates and the nickel hydroxide nanosheets for the Auger measurements. Figure 2(c) shows the Auger spectra for different annealing temperatures in vacuum. Comparing the results for different annealing temperatures, the signal from oxygen (O) around 500 eV was apparently suppressed at 250 ℃. Although the small oxygen signal seems to be remained at 250 ℃, it is difficult to perfectly remove signals originated from surface contaminants even in UHV chamber. The element specific XANES measurement reveals that the 250 ℃ sample does not contain the multiple oxide/hydroxide signal. Hence, we can conclude that the remained oxygen atoms observed in the Auger measurement at 250 ℃ do not have chemical bonds to nickel atoms. The result implies that water molecule dissociations from the hydroxide nanosheets accompany with oxygen molecule dissociations, which lead to crystallizations of nickel metal.
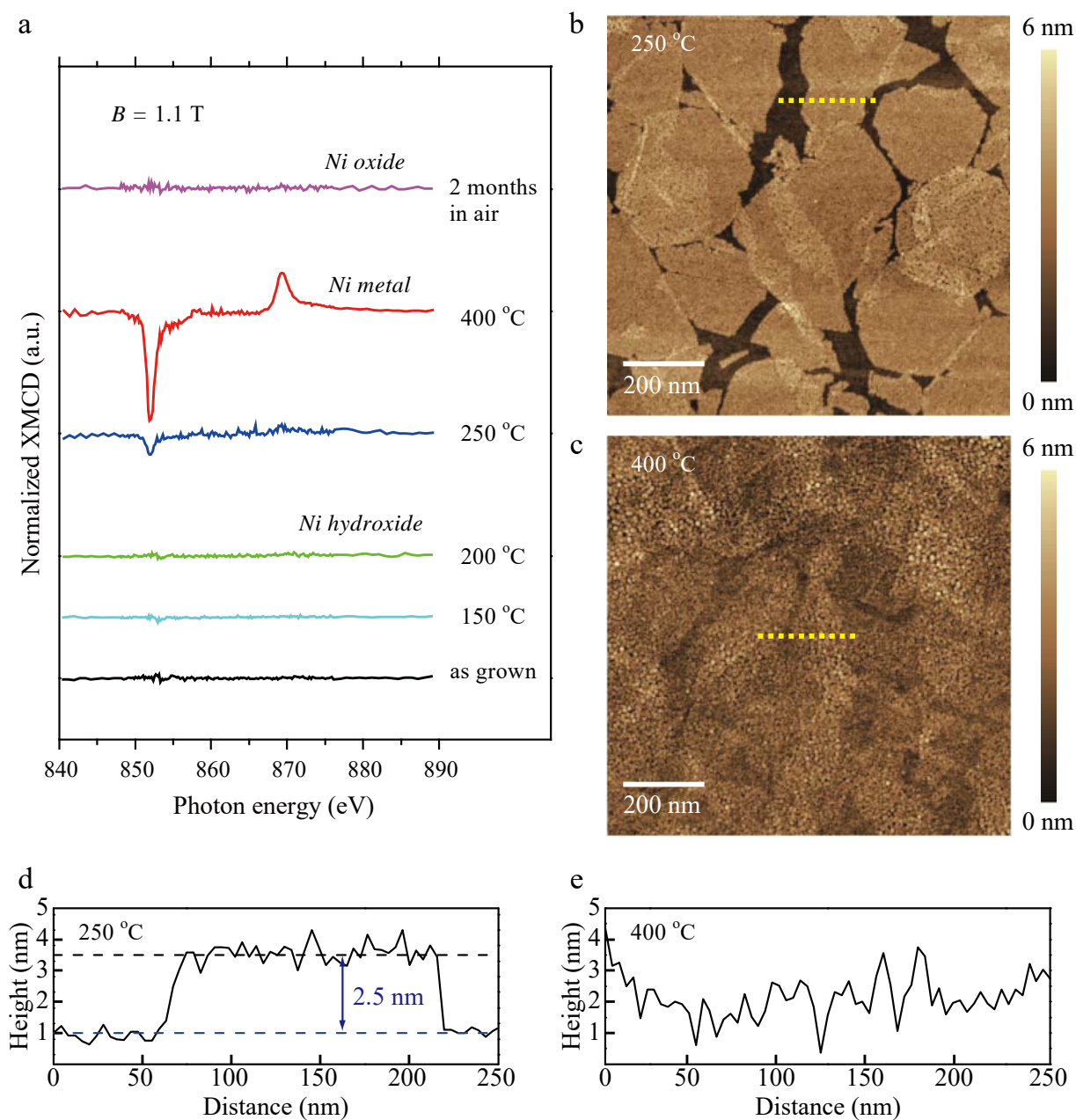
Figure3. (a) Normalized X-ray magnetic circular dichroism (XMCD) spectra for different annealing temperatures. (b) Atomic force microscopy image of the sample annealed at 250 ℃. (c) Atomic force microscopy image of the sample annealed at 400 ℃. (d) Height profile along the dashed line marked in (b). (e) Height profile along the dashed line marked in (c).

XMCD measurements also support the transition from the nickel hydroxide to the nickel metal.

Figure 3(a) shows XMCD spectra normalized by the amplitude of L_3 peak in each X-ray

absorption spectra. A weak XMCD signal appeared in the sample annealed at 250 °C and was

enhanced in the sample annealed at 400 °C, which means a ferromagnetic order induced by the metallization.

To evaluate the amplitude difference in the XMCD signal, we compared surface morphologies between the samples annealed at different temperatures by an atomic force microscopy. Since the measurements were carried out at ambient air, surface oxidations may have occurred. Nevertheless, the morphologies shown in Fig. 3(b)(c) were significantly different. For the case of the sample annealed at 250 °C, the initial sheet structures were still remained even after the metallization as shown in Fig. 3(d). The height between the substrate surface and the top of the 1st layer increased from 1.8 nm to 2.5 nm by the annealing at 250 °C. It should be pointed out that the increase in the measurement height may originate from surface oxidations. In contrast, nickel atoms widely diffused on the substrate at 400 °C, leading to formations of nickel nanoparticles. The surface roughness increases about twice as that of the sample annealed at 250 °C as shown in Fig. 3(e).

From the XMCD spectra, we can estimate magnetic moments per Ni atom by calculation based on the sum rules [34]. Assuming the number of unoccupied d states $n_h = 1$ and neglecting the contribution of the spin magnetic dipole operator, the total magnetic moments for the samples annealed at 250 °C and at 400 °C are estimated to be 0.03 μ_B and 0.24 μ_B, respectively. These are smaller than the reported value of bulk nickel ~ 0.6 μ_B. Reductions of total magnetic moments due to interactions with substrates have been observed in thin nickel films [25-27]. In our XMCD measurements, the direction of the external magnetic field of 1.1 T was perpendicular to the sample, so that the magnetic moments were not fully aligned along the magnetic field especially in thinner 250 °C sample. Another possibility is a reduction of the Curie temperature,

which is strongly dependent on the thickness [35]. These are the reasons why the XMCD signal measured at room temperature was relatively weak for the sample annealed at 250 °C even though the X-ray absorption spectra revealed the metal transition.

Conclusions

Chemically exfoliated Ni(OH)$_2$ nanosheets are converted into metallic nickel 2D structure by annealing above 250 °C in vacuum. XANES signal significantly changes from a multiple structure to a broad metallic structure. Auger measurement also supports the metallic transition accompanied with dissociation of oxygen. XMCD measurement reveals that the converted metal structures exhibit ferromagnetic behavior. The perpendicular magnetization increases with the annealing temperature due to the structural change from 2D-like sheet to nanoparticle.

Acknowledgements

References

[1] Geim A K and Grigorieva I V 2013 *Nature* **499** 419-425

[2] Novoselov K S, Mishchenko A, Carvalho A and Castro Neto A H 2016 *Science* **353** aac9439

[3] Wang F, Wang Z, Shifa T A, Wen Y, Wang F, Zhan X, Wang Q, Xu K, Huang Y, Yin L, Jiang C and He J 2017 *Adv. Func. Mater.* **27** 1603254

[4] Ma Y, Li B and Yang S 2018 *Mater. Chem. Front.* **2** 456-467

[5] Luo M, Yang Y, Sun Y, Qin Y, Li C, Li Y, Li M, Zhang S, Su D and Guo S 2019 *Mater. Today* **23** 45-56

[6] Han G H, Duong D L, Keum D H, Yun S J and Lee Y H 2018 *Chem. Rev.* **118** 6297-6336

[7] Ma R and Sasaki T 2010 *Adv. Mater.* **22** 5082-5104

[8] Fukuda K, Sato J, Saida T, Sugimoto W, Ebina Y, Shibata T, Osada M and Sasaki T 2013 *Inorg. Chem.* **52** 2280-2282

[9] Funatsu A, Tateishi H, Hatakeyama K, Fukunaga Y, Taniguchi T, Koinuma M, Matsuura H and Matsumoto Y 2014 *Chem. Commun.* **50** 8503-8506

[10] Ida S, Shiga D, Koinuma M and Matsumoto Y 2008 *J. Am. Chem. Soc.* **130** 14038-14039

[11] Ida S, Takashiba A and Ishihara T 2013 *J. Phys. Chem. C* **117** 23357-23363

[12] Awaya K, Kawahara S, Matsuda J, Ishihara T, Koinuma M and Ida S in preparation

[13] Wang Q and O'Hare D 2012 *Chem. Rev.* **112** 4124-4155

[14] Long X, Wang Z, Xiao S, An Y and Yang S 2016 *Mater. Today* **19** 213-226

[15] Wei X-L, Tang Z-K, Guo G-C, Ma S and Liu L-M 2015 *Sci. Rep.* **5** 11656

[16] Tang Z-K, Liu W-W, Zhang D-Y, Lau W-M and Liu L-M 2015 *RSC Adv.* **5** 77154-77158

[17] Tkalych A J, Yu K and Carter E A 2015 *J. Phys. Chem. C* **119** 24315-24322

[18] Nagli M and Toroker M C 2018 *Solid State Ionics* **314** 149-155

[19] Nagli M and Toroker M C 2018 *J. Chem. Phys.* **149** 141103

[20] Bode H, Dehmelt K and Witte J 1966 *Electrochim. Acta* **11** 1079-1087

[21] Hall D S, Lockwood D J, Bock C and MacDougall BR 2015 *Proc. R. Soc. A* **471** 20140792

[22] Soriano L, Abbate M, Vogel J, Fuggle JC, Fernández A, González-Elipe A R, Sacchi M and Sanz J M 1993 *Chem. Phys. Lett.* **208** 460-464

[23] Jiang J, Sun F, Zhou S, Hu W, Zhang H, Dong J, Jiang Z, Zhao J, Li J, Yan W and Wang M 2018 *Nat. Commun.* **9** 2885

[24] Chen C T, Sette F, Ma Y and Modesti S 1990 *Phys. Rev. B* **42** 7262-7265

[25] Vogel J, Panaccione G and Sacchi M 1994 *Phys. Rev. B* **50** 7157-7160

[26] Srivastava P, Wilhelm F, Ney A, Farle M, Wende H, Haack N, Ceballos G and Baberschke K 1998 *Phys. Rev. B* **58** 5701-5706

[27] Dhesi S S, Dürr H A, Laan G, Dudzik E and Brookes N B 1999 *Phys. Rev. B* **60** 12852-12860

[28] Liang Z-H, Zhu Y-J and Hu X-L 2004 *J. Phys. Chem. B* **108** 3488-3491

[29] Zhu J, Gui Z, Ding Y, Wang Z, Hu Y and Zou M 2007 *J. Phys. Chem. C* **111** 5622-5627

[30] Qi Y, Qi H, Li J and Lu C 2008 *J. Cryst. Growth* **310** 4221-4225

[31] Kuang D-B, Lei B-X, Pan Y-P, Yu X-Y and Su C-Y 2009 *J. Phys. Chem. C* **113** 5508-5513

[32] Zhang X, Shi W, Zhu J, Zhao W, Ma J, Mhaisalkar S, Maria T L, Yang Y, Zhang H, Hng H H and Yan Q 2010 *Nano Res.* **3** 643-652

[33] Kuang Y, Feng G, Li P, Bi Y, Li Y and Sun X 2016 *Angew. Chem. Int. Ed.* **55** 693-697

[34] Chen C T, Idzerda Y U, Lin H-J, Smith N V, Meigs G, Chaban E, Ho G H, Pellegrin E and Sette F 1995 *Phys. Rev. Lett.* **75** 152-155

[35] Huang F, Kief M T, Mankey G J, Willis R F 1994 *Phys. Rev. B* **49** 3962-3971